*Article*

# Efflorescent Sulphates with M⁺ and M²⁺ Cations from Fumarole and Active Geothermal Fields of Mutnovsky Volcano (Kamchatka, Russia)

Elena S. Zhitova [1],*, Dmitry A. Khanin [2], Anton A. Nuzhdaev [1], Maria A. Nazarova [1], Rezeda M. Ismagilova [3], Vladimir V. Shilovskikh [4], Anastasia N. Kupchinenko [1], Ruslan A. Kuznetsov [1] and Pavel S. Zhegunov [1]

[1]  Institute of Volcanology and Seismology, Russian Academy of Sciences, Bulvar Piypa 9, Petropavlovsk-Kamchatsky 683006, Russia; nuzhdaev@gmail.com (A.A.N.); nazarovamar@mail.ru (M.A.N.); kupchasta@yandex.ru (A.N.K.); ruslanalexeevich@yandex.ru (R.A.K.); pavel.zhegunov@bk.ru (P.S.Z.)
[2]  Institute of Experimental Mineralogy, Russian Academy of Sciences, Academica Osypyana ul. 4, Chernogolovka 142432, Russia; mamontenok49@yandex.ru
[3]  Department of Crystallography, St. Petersburg State University, Universitetskaya Nab. 7/9, St. Petersburg 199034, Russia; rezeda.m.ismagilova@gmail.com
[4]  Department of Colloid Chemistry, St. Petersburg State University, Universitetskaya Nab. 7/9, St. Petersburg 199034, Russia; vova_bel@mail.ru
*  Correspondence: zhitova_es@mail.ru

**Abstract:** In this study, sulphate efflorescent minerals covering the surface of the Donnoe and Dachnoe fields of the Mutnovsky volcano are described. The minerals were precipitated on the argillic facies as the result of water–rock interaction and fumarole emission. A chemical composition of Ca, Ba, $(NH_4)^+$, $Na$-$Fe^{3+}$, $(NH_4)^+$-$Al$, $(NH_4)^+$-$Fe^{3+}$, $Na$-$Al$, $K$-$Al$, and $K$-$Fe^{3+}$ sulphates was reported. Elements such as Sr, Mg, Co, Ni, Ti and P were found as isomorphic impurities. Ammonia species were concentrated around fumaroles. The mineral assemblage described herein is unique in relation to other geological settings and reflects the process of low-temperature mineral formation associated with volcanism. The thermal water contains cations such as H, Na, K, $NH_4$, Ca, Mg, $Fe^{2+}$, $Fe^{3+}$, and Al in different proportions with pH ranging from 2.4 to 6.5 and the dominance of acidic waters. The gas condensate bears such cations as $(NH_4)^+$, Ca, and Mg and has a pH of ~5. Thus, the rest of the main cations are derived from the leaching of the host rocks. Among the identified phases, the alunite-supergroup minerals are more prone to isomorphism. The Ti, Co, and Ni impurities mark the unique geochemistry of thermal water at the Mutnovsky volcano. We postulate that the chemical composition of alunite-supergroup minerals reflects the types of hydrothermal occurrences and contains important information on the geochemistry of the hydrothermal process.

**Keywords:** jarosite; alunite; alum; amarillite; tschermigite; lonecreekite; volcano; geothermal field; fumarole; thermal water; steam-emitting vent; Mutnovsky; Kamchatka; hot spring; efflorescence

## 1. Introduction

The mineralogy of active fumaroles and geothermal fields is interesting from several different points of view. These geological settings can be considered integral companions of active volcanism, which is supposed to take place from the moment plate tectonics appeared. Fumaroles and gas-steam vents (common at geothermal fields) mark tectonically weakened zones and are responsible for the flow of deep elements (magmatic and/or from host rocks) to the day surface. High temperatures and the presence of aggressive fluids lead to the transformation of the initial rocks, the redistribution of chemical elements, and the formation of a definite mineral association depending on many thermodynamic and physicochemical characteristics of the environment.

In volcano-hydrothermal systems, acidic waters are produced due to the interaction of volcanic gases $SO_2$, $H_2S$, and HCl with water, resulting in $H^+$ release [1–3]. The circulation

of acidic solution produces leaching of host rocks and remobilization of the elements contained in them, as well as fumarole-emitted elements that lead to the formation of efflorescent minerals that have been the subjects of recent investigations [4–8]. Efflorescent minerals often form finely dispersed poorly crystalline material, intergrowths, which makes it difficult to reliably determine such phases. This is the defining issue for the lack of mineralogical data on the efflorescence of most hydrothermal systems, in particular Kamchatka (Far Eastern Russia). Although such minerals play an important role in the life of the hydrothermal system, scientists generally emphasize the importance of the results of studies on efflorescent minerals for the exploration of Mars, since sulphate-rich mineral associations have been found there [4–6,8]. In particular, in this work, we present the chemical compositions of the alunite-group minerals identified in the efflorescence of the thermal fields of the Mutnovsky volcano, which attract the attention of researchers in the context of the study of Mars. For instance, the finding of jarosite on Mars [9–11] actualized the study of a variety of its aspects: formation conditions [12], thermodynamic stability [13], atomic arrangement at low temperature [14], and band assignment at visible and infrared spectra [15–17]. This increased interest in the study of minerals of the alunite group indicates that our data can be used in the study of the mineralogy of other planets and other objects of the solar system. In particular, the mineral association discovered by us is unique and reflect the geochemical conditions of low-temperature active geothermal and fumarole fields. If such an association of minerals is found, say, on Mars, this would indicate the presence of hydrothermal activity on the surface of the planet in the past.

The present work aims to describe the surface sulphate efflorescence with K, Na, Ba, NH$_4$, and Ca that precipitated from thermal water and fumarolic gas condensate at two different localities: the Dachnoe thermal field and the Donnoe fumarole field (both associated with the Mutnovsky volcano in Kamchatka, Russia). The description of geochemical conditions is based on our field documentation and the previously reported results on the hydrogeochemistry of the Donnoe fumarole field [18]. Knowledge of the mineral parageneses formed at the fumarole and geothermal fields can be applied in various areas of geology. For example, the transport and concentration of chemical elements are relevant for ecology, geochemistry, and ore geology and may provide information about deep magmatic bodies, the heat of which can be potentially explored as a geothermal energy source.

Finally, we note that the mineral association described in this work is close (but not identical) in element composition to the associations formed in environments such as acid mine drainage (AMD) [19,20] and burning coal heaps [21,22]. Thus, the results obtained in this work may be of interest for comparison with other non-volcanic environments.

## 2. Materials and Methods

### 2.1. Geological Setting

South Kamchatka is a part of the Kuril-Kamchatka island arc system, articulated in the north with the Aleutian arc, and in the southwest with the Japanese arc. Similar to other island arcs, it is characterized by high tectonic-magmatic activity, which is expressed on the surface by modern volcanism. Seventy kilometers south of Petropavlovsk-Kamchatsky, there is an area where intense and varied volcanic activity is widespread. The Mutnovsky volcano is located in this area (Figure 1a). Mutnovsky is a Middle Pleistocene thyroid basalt volcano representing a complex uneven-aged massif (Figure 1b,c). This is one of the most active volcanoes in South Kamchatka. The area of Mutnovsky is located within the regional sub-deep fault zone, at the junction of the asymmetric step depression of the volcanic zone of South Kamchatka with the uplift of the Eastern horst-anticlinorium [23]. In the Mutnovsky district, several types of modern thermal manifestations can be distinguished:

1. The active funnel of the Mutnovsky volcano, where the measured temperature reached 750 °C in the 1960s [23–25], 570–600 °C in 2000–2005 [26–28], and 620 °C in 2006 [29].

2. Fumarole fields of the northern crater of the Mutnovsky volcano: Verkhnee and Donnoe, where the measured temperatures reached 300 °C and 320 °C in 1974, respectively [23], and 150 °C on Donnoe in the 2000s [28].
3. Thermal fields of the Severo-Mutnovsky volcano-tectonic zone: Severo-Mutnovsky, Dachnoe, and Verkhnezhirovskiy, with temperatures up to 110 °C [23].
4. Sources of overheated waters: Nizhnezhirovskie and Voinovskie, where temperatures have never been reported higher than 100 °C [23].
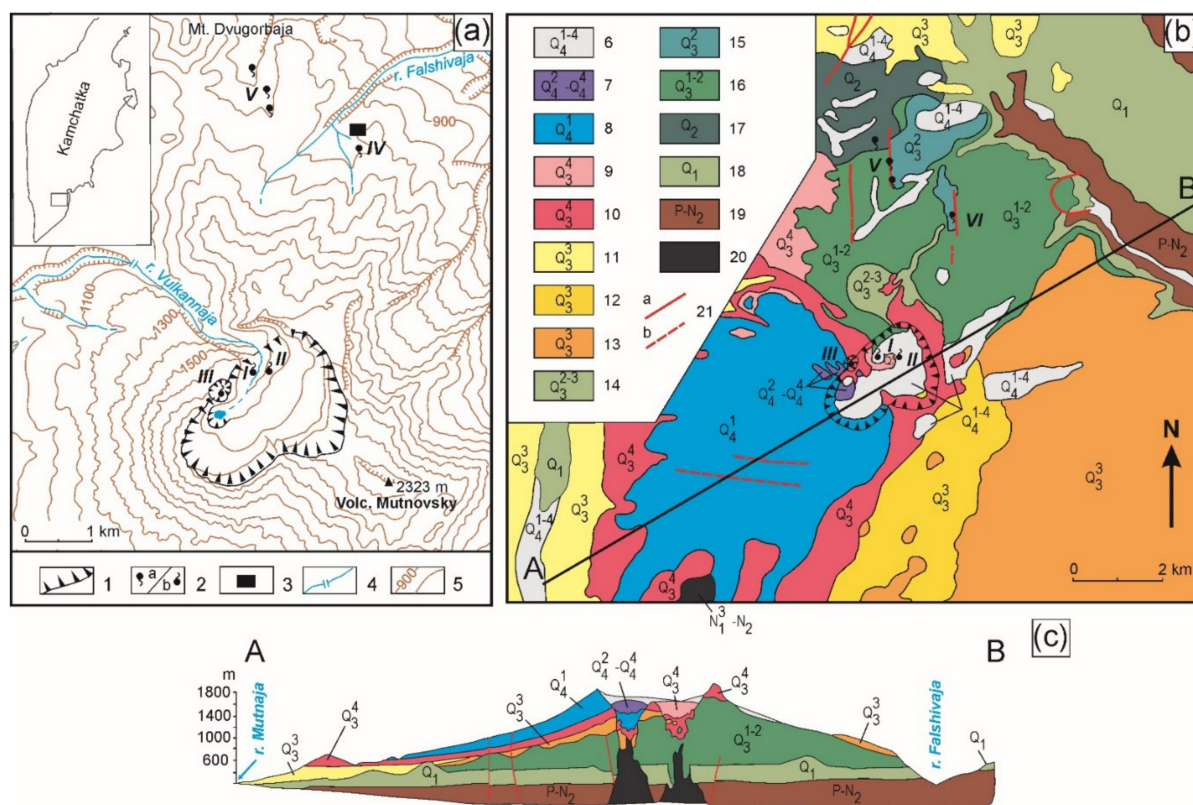


**Figure 1.** The scheme of the Mutnovsky volcano area (**a**), geological map (**b**) and (**c**) representative A-B (line) cross-section (modified after [23]). Symbols: 1—scarps of craters and calderas of Mutnovsky volcano; 2—the largest thermal manifestations (a—thermal fields; b—fumarole fields); 3—Mutnovsky geothermal power plant; 4—rivers; 5—contours of the relief; 6—modern and undissected Holocene sediments (alluvium, deposits of rockslides, mudflows, lahars, glaciers and glacial sediments); 7—basalts, andesite-basalts, tuffs, and volcanic scoria (8.9 ka BP-present); 8—basalts (10.1–8.9 ka BP); 9—dacite pumice of the caldera-forming eruption of Mutnovsky volcano; 10—basalts; 11—dacite, andesidacite, andesite pumice and ignimbrites from the main stage of the caldera-forming eruptions of Gorely volcano; 12—caldera lake deposits and lava-pyroclastic formations; 13—lava-pyroclastic formation of the basalt-andesite-dacite-rhyolite series; 14—lava flows and residual outcrop of stratovolcanoes basalts, andesites, dacite pumice, and ignimbrites; 15—side breakthroughs and monogenic volcanoes of the precaldera stage; 16—lava-pyroclastic formation of the basalt-andesite-dacite-rhyolite series; 17—basalt-andesite-dacite-rhyolite formation of the pre-caldera structure of Gorely volcano; 18—caldera lake deposits and lava-pyroclastic formations; 19—basement-dislocated strata of green-metamorphosed and silicified volcanic and volcanogenic-sedimentary deposits of the Pribrezhnyj formation and slightly dislocated strata of contrasting volcanites of the basalt-rhyolite series with extrusions and subvolcanic bodies of the Yuzhno-Bystrinskj formation; 20—effusive domes, extrusions, subvolcanic bodies, and lava vents, in section—basalts, andesite-basalts, andesites, dacites, and rhyolites; 21—(a) faults with defined displacement and (b) asymmetric, damped, and buried; I—Donnoe fumarole field; II—Verkhnee fumarole field; III—active funnel; IV—Dachnoe thermal field; V—Severo-Mutnovsky thermal fields. The arrow in (**b**) shows the North direction.

In this work, we consider minerals sampled within the Donnoe fumarole field of the Northern crater of the Mutnovsky volcano (Figure 1a) and within the Southern group of the Dachnoe geothermal field.

The Donnoe fumarole field is located close to the active funnel of the Mutnovsky volcano (the active crater of the volcano). It is located on the smooth surface (Figure 2a) and the temperature at a depth of 20 cm is 20–110 °C. The temperature of the hottest fumaroles are about 120–150 °C. The Donnoe fumarole field is a former boiling crater lake, which was a solution of hydrochloric and sulfuric acids with a pH < 1. The lake existed until 1956 and ceased to exist as a result of a breakthrough of the crater wall.
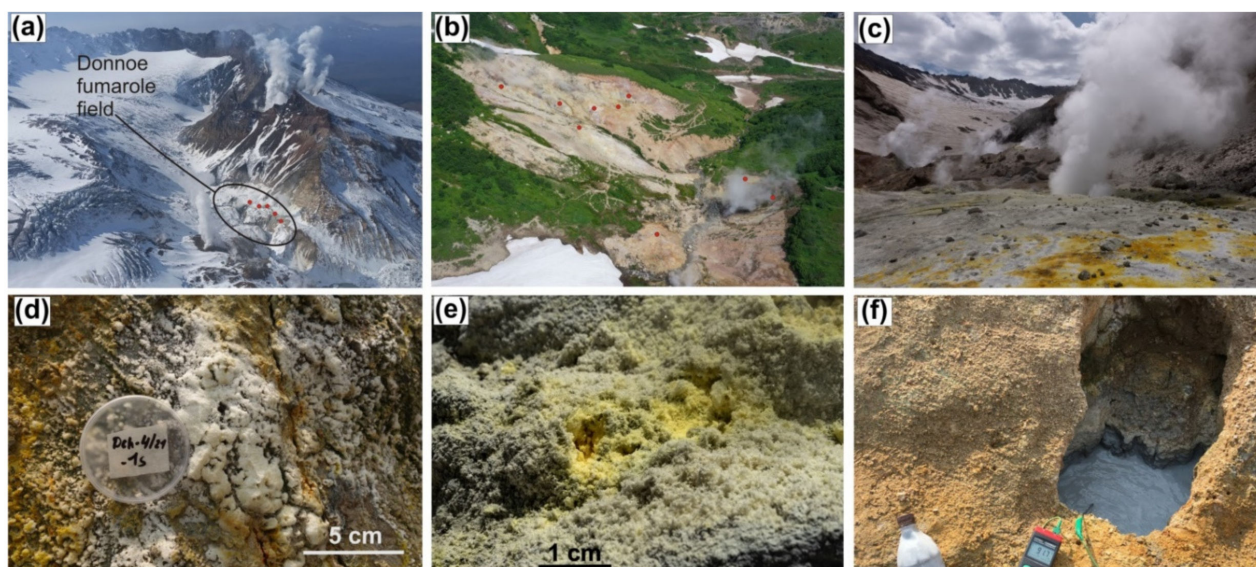


**Figure 2.** Sampling schemes of Donnoe fumarole field (**a**), Dachnoe thermal field (**b**), the view to Donnoe fumarole field (**c**), efflorescent minerals from Dachnoe thermal field (**d**), and Donnoe fumarole field (**e**), bubbling pools from Dachnoe thermal field (**f**).

The Dachnoe thermal field (also known as the small geyser field) is located on the slope of the Mutnovsky volcano (Figure 2b), 8 km north from the Donnoe fumarole field. It is located in a rounded basin with steep walls up to 30 m high. The geothermal activity is realized through gas-steam vents, bubbling pools, and steaming ground. The temperature of gas-steam vents does not exceed 99 °C.

In the area around the Dachnoe thermal field, pumice tuffs of dacitic composition come to the surface (Figure 1b). Below the pumice tuffs of the area of Dachnoe lies the lava-pyroclastic complex of the Dvugorby volcano, which is represented by tuffs and tuff breccias from basic to acidic composition ($Q_2$-$Q_3$). They are underlain by deposits of the Skalisty volcano: basalts, basaltic andesites, their tuffs, and tuff breccias ($Q_2$-$Q_3$). The ignimbrites of the Gorely volcano ($Q_2$-$Q_3$) occur below [30]. The surface of the field itself is composed of argillic alteration that is the product of host (primary) rock alteration by volcanic gases and thermal water. The argillic facies surface is covered by efflorescent minerals.

The Donnoe (in some references the name is translated as "Bottom") fumarole field is located in the caldera of the Mutnovsky volcano. The Mutnovsky volcano is composed of rocks in the basalt-andesite-rhyodacite series; modern rocks have a basaltic composition. Basalts, andesite-basalts, andesites, their tuffs, and tuff breccias of the Zhirovsky volcano ($Q_1$), underlain by volcanic rocks of the Yuzhnobystrinsky andesite-basalt-andesite and Pribrezhny basalt-andesite volcanic complexes (P-$N_2$) serve as the foundation of the modern volcanic edifice of Mutnovsky volcano [31] (Figure 1b). On the territory of the field, the primary rocks are altered to argillic facies forming the day surface. Efflorescent minerals grow on the argillic facies.

### 2.2. Materials and Sample Preparation

The mineral samples studied in this work were collected from the surface of the Donnoe fumarole field and Dachnoe thermal field (Mutnovsky volcano) (Figure 2c–f), in particular, from heated ground areas (temperature 40–65 °C), near steam-emitting vents (~70 °C) and fumarole (~120 °C). At both thermal sites, the samples are represented by white, yellow, and ochre yellow efflorescent minerals and crust.

The samples were partly ground in an agate mortar and investigated by powder X-ray diffraction. The other parts of the samples were mounted in epoxy blocks and polished using a set of diamond pastes; these samples were carbon-coated and studied with scanning electron microscopy (SEM) and energy-dispersive X-ray spectroscopy (EDS).

Water samples were collected from bubbling pools and filtered through a membrane with a porosity of 0.45 μm into sterile plastic bottles with a volume of 1 L. The condensates of the steam-emitting vents were sampled by forced pumping with cooling; the sample volume was 1 L. The main physicochemical parameters were measured with portable Hanna pH meters (pH measurement accuracy ±0.1). The temperature was measured with a k-type thermocouple (±0.1 °C).

### 2.3. Methods

The phase analyses of samples were carried out with the powder X-ray diffractometer Shimadzu XRD-7000 using the following conditions: Cu$K\alpha$ radiation, 30 kV/30 mA, scan speed 1°/min, step width 0.1°, and 2-theta range 5–65° and the powder X-ray diffractometer Rigaku Miniflex II with Cu$K\alpha$ radiation at 30 kV/15 mA, scan speed 1°/min, step width 0.1°, and 2-theta range 4–60°. The data were processed using ICDD database. The samples available in small quantities were subjected to X-ray diffraction using a Rigaku R-Axis Rapid II diffractometer equipped with a curved image plate detector and a rotating anode X-ray source with Co$K\alpha$ radiation, scan speed 1°/min, step width 0.02°, and 2-theta range 5–70°. The data were integrated using the software package Osc2Tab/SQRay [32]. All X-ray diffraction powder analyses were carried out at room temperature. In total, 35 samples were subjected to powder X-ray diffraction.

The chemical composition was analyzed using SEM Camscan MV2300, nanoampermeter, and INCA Energy 450 EDS (Oxford Instruments Ltd., Great Britain) and SEM Hitachi S3400N equipped with an Oxford X-Max 20 EDS (Oxford Instruments Ltd., Great Britain). The operation conditions (for Camscan/Hitachi) were an accelerating voltage of 15/20 kV and a beam current of 30/1.5 nA and the spectra were obtained at spot mode for 70/30 s each. The following standards were used (Camscan/Hitachi): Na—chkalovite/albite, Mg—diopside/MgO, Al—tremolite/albite, Si—chkalovite/albite, P—synthetic $KTiPO_5$/InP, S—$SrSO_4$/$FeS_2$, K—potassium feldspar/KCl, Ca—diopside/$CaSO_4$, Ti—synthetic $FeTiO_3$/Ti, Fe—hornblende/$FeS_2$, Co—synthetic CoAsS/Co, Ni—synthetic NiO/Ni, Sr—$SrSO_4$/$SrF_2$, Ba—synthetic $BaSO_4$/$BaF_2$, and N—BN. The uncertainty of a single measurement did not exceed 0.1/0.3 wt. %. The advantages of energy-dispersive (ED) spectrometer application are the possibility of analyzing small-size grains of distinct minerals found in tight association and completion of chemical analyses in a short time. Both short-time and low-probe current significantly contribute to non-distraction of the studied material (see, e.g., [33]).

In total, about 1000 chemical analyses were obtained from polished sections, of which about 220 analyses contained considerable content of S, Na, K, Ca, and/or Ba, i.e., corresponded to sulphates of alkali and alkali earth elements. These analyses were grouped by the content of chemical elements. The analyses of each group were averaged and used to calculate the ratios between the elements.

When studying the composition of hydrothermal waters, the following analytical methods (complete chemical analysis) were used: potentiometric (pH, HCO, and F); photometric ($SO_4$, $NH_4$, Al, $SiO_2$ and Fe); titrimetric (Cl); atomic absorption spectrophotometric (Ca and Mg); flame emission spectrophotometry (Na, K, and Li).

## 3. Results

### 3.1. Powder X-ray Diffraction

The bulk composition of efflorescent minerals from the Donnoe fumarole field is represented by halotrichite, alunogen, gypsum, native sulphur, melanterite, mascagnite, letovicite, and alunite-type minerals. The efflorescent from the Dachnoe thermal field is composed of halotrichite, alunogen, gypsum, alum- and alunite-type minerals, copiapite group mineral, and melanterite. In both cases, alunite-type minerals are closely associated with alunogen. The detailed information showing phase analyses, *d*-values, line intensity and *hkl* for six representative samples is given in Table S1. Figure 3 shows a schematic visual representation of the results from the Table S1. Table 1 lists identified sulphates relative to the frequency of their occurrence in samples.
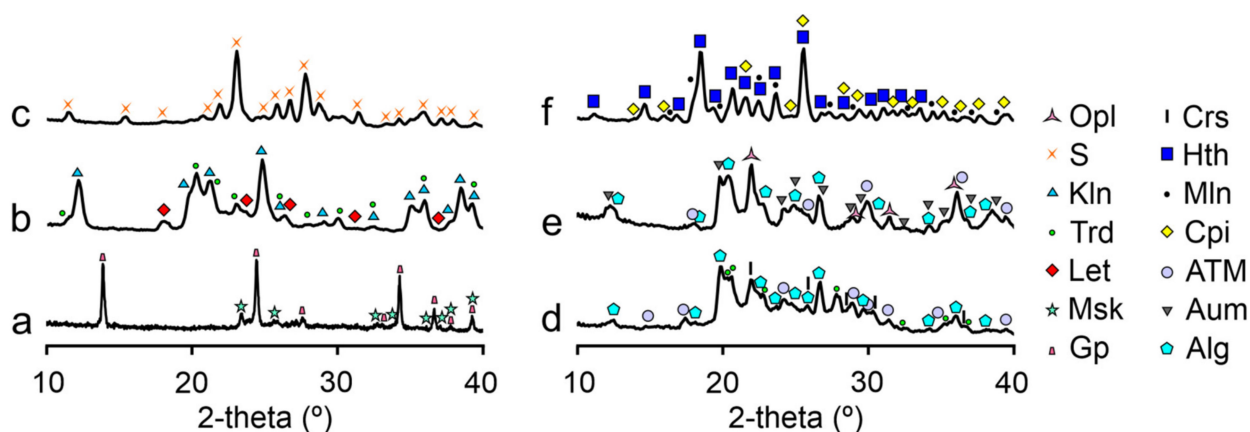


**Figure 3.** Powder X-ray diffraction patterns of efflorescent minerals from Donnoe fumarole field (**a–c**) and Dachnoe thermal field (**d–f**). Hth—halotrichite, Mln—melanterite, Cpi—copiapite, ATM—alunite-type compounds, Aum—alum, Alg—alunogen, Opl—opal, S—native Sulphur, Kln—kaolinite, Trd—tridymite, Crs—crystoballite, Let—letovicite, Msk—mascagnite, Gp—gypsum.

**Table 1.** Sulphate efflorescence minerals from Mutnovsky volcano detected by powder X-ray diffraction analyses.

| Mineral, Ideal Chemical Formula | Donnoe Fumarole Field | Dachnoe Thermal Field |
|---|---|---|
| Halotrichite, $Fe^{2+}Al_2(SO_4)_4 \cdot 22H_2O$ | **** | **** |
| Alunogen, $Al_2(SO_4)_3 \cdot 17H_2O$ | *** | *** |
| Gypsum, $CaSO_4 \cdot 2H_2O$ | ** | *** |
| Alum-type minerals, $A^+M^{3+}(SO_4)_2 \cdot 12H_2O$ | - | ** |
| Alunite-type minerals, $DG_3(TX_4)_2X'_6$ | * | * |
| Melanterite, $Fe^{2+}(H_2O)_6SO_4 \cdot H_2O$ | * | * |
| Copiapite-group mineral, $M^{2+}Fe^{3+}_4(SO_4)_6(OH)_2 \cdot 20H_2O$ | - | * |
| Letovicite, $(NH_4)_3H(SO_4)_2$ | * | - |
| Mascagnite, $(NH_4)_2SO_4$ | * | - |

The number of asterisks indicates the frequency of the mineral occurrence in the analyzed samples: ****—very widespread; ***—common; **—regular; and *—rare.

According to phase analyses by powder X-ray diffraction, kaolinite is found in tight association with efflorescent minerals since it is the substrate on which and from which these minerals grow.

It is tempting to divide identified minerals into separate associations and correlate them with the processes of either acidic alteration or fumarole emission. However, such

a division is impossible due to the complexity of the natural process. The mineralogy of the efflorescent is heterogeneous and changes on a centimeter scale. However, we report some tendencies: ammonium minerals concentrate close to gas-emitting fumaroles or vents, letovicite is found in association with kaolinite and tridymite, and mascagnite is associated with gypsum. The following main associations were found: (i) halotrichite and alunogen; (ii) alunogen and kaolinite; (iii) halotrichite, melanterite, and copiapite-group mineral, (iv) tschermigite/lonecreekite (alum-type minerals), alone or with alunogen; (v) gypsum; (vi) native sulphur; (vii) alunogen, gypsum, and alunite-type minerals; (viii) halotrichite and alunite-type minerals. All sulphate minerals can be found in association with underlying clay minerals and/or rather abundant $SiO_2$ or $SiO_2 \times nH_2O$ polymorphs: opal, tridymite, and cristobalite, all derived as the result of an alteration of silicates.

### 3.2. Energy-Dispersive Spectroscopy

The energy-dispersive spectroscopy data agree with powder X-ray diffraction analyses: Fe-Al, Fe and Al sulphates are abundant in the studied samples. Apart from sulphates, silicates corresponding to the remnants of the initial magmatic rocks converted to argillite as a result of hydrothermal activity are found in association with sulphates. In addition, the samples contain pyrite crystals and $SiO_2$ or $SiO_2 \times nH_2O$ polymorphs. The chemical composition of Na-, K-, Ca-, Ba-, and ($NH_4$)-sulphates are given in Tables 2 and 3.

**Table 2.** Chemical composition of baryte, gypsum, and alunite supergroup minerals: jarosite, alunite, natrojarosite and natroalunite.

| Wt.% | Baryte | Gypsum | | Jarosite | Alunite | Na-Rich Jarosite | K-Rich Natrojarosite | Natro-Alunite | Natrojarosite | |
|---|---|---|---|---|---|---|---|---|---|---|
| Location | Dachnoe | Donnoe | Dachnoe | | | Donnoe | | | Donnoe | Dachnoe |
| $n$ | 6 | 41 | 16 | 13 | 17 | 9 | 23 | 17 | 12 | 16 |
| $Na_2O$ | n.d. | n.d. | n.d. | 1.25 | 1.28 | 3.15 | 3.08 | 5.04 | 3.96 | 4.74 |
| $K_2O$ | n.d. | n.d. | n.d. | 6.55 | 6.77 | 4.91 | 4.55 | 1.87 | 1.81 | 0.77 |
| CaO | n.d. | 32.28 | 32.67 | 1.65 | 0.52 | 0.25 | 0.43 | 0.17 | 0.04 | 0.08 |
| SrO | 1.19 | n.d. | n.d. | 0.29 | 1.72 | n.d. | n.d. | 0.05 | 0.09 | n.d. |
| BaO | 61.55 | n.d. | n.d. | 0.05 | 0.49 | n.d. | n.d. | n.d. | n.d. | n.d. |
| MgO | 0.20 | n.d. | 0.07 | 0.16 | 0.02 | 0.07 | 0.12 | 0.07 | 0.20 | 0.42 |
| FeO [1] | n.d. | 0.49 | 0.37 | n.d. | n.d. | n.d. | n.d. | n.d. | n.d. | n.d. |
| CoO | n.d. | n.d. | n.d. | 0.22 | 0.07 | 0.23 | 0.26 | 0.11 | 0.31 | n.d. |
| NiO | n.d. | n.d. | n.d. | 0.10 | 0.04 | 0.11 | n.d. | 0.04 | n.d. | n.d. |
| $TiO_2$ | n.d. | n.d. | n.d. | n.d. | n.d. | 0.12 | 0.25 | 0.04 | 0.22 | 0.44 |
| $Al_2O_3$ | n.d. | n.d. | n.d. | 6.92 | 28.18 | 6.53 | 5.31 | 25.15 | 4.77 | 5.55 |
| $Fe_2O_3$ [1] | n.d. | n.d. | n.d. | 36.67 | 10.29 | 38.72 | 39.36 | 15.91 | 41.11 | 39.19 |
| $SO_3$ | 36.00 | 47.81 | 47.16 | 32.92 | 34.72 | 33.34 | 32.14 | 37.20 | 33.25 | 33.97 |
| $P_2O_5$ | n.d. | n.d. | n.d. | 0.68 | 2.77 | 0.26 | 0.37 | 0.21 | 0.57 | 0.93 |
| $H_2O$ [2] | n.d. | 21.05 | 21.12 | 10.86 | 12.30 | 11.15 | 11.05 | 12.54 | 11.16 | 11.08 |
| $(NH_4)_2O$ [3] | n.d. | n.d. | n.d. | n.d. | n.d. | n.d. | n.d. | 0.69 | 0.81 | 0.9 |
| Total | **98.95** | **101.63** | **101.39** | **98.32** | **99.16** | **98.82** | **97.53** | **99.04** | **98.76** | **98.07** |
| | | | | *apfu* calculated on the basis of | | | | | | |
| | $\Sigma cat + S = 2$ | Ca + Fe = 1 | | | | Fe + Al + Mg + Co + Ni = 3 | | | | |
| Na | n.d. | n.d. | n.d. | 0.20 | 0.18 | 0.49 | 0.49 | 0.70 | 0.62 | 0.75 |
| K | n.d. | n.d. | n.d. | 0.69 | 0.63 | 0.50 | 0.47 | 0.17 | 0.19 | 0.09 |
| Ca | n.d. | 0.99 | 0.99 | 0.15 | 0.04 | 0.01 | 0.04 | 0.01 | 0.04 | 0.01 |
| Sr | 0.03 | n.d. | n.d. | 0.01 | 0.07 | n.d. | n.d. | 0.00 | 0.00 | n.d. |
| Ba | 0.93 | n.d. | n.d. | 0.00 | 0.01 | n.d. | n.d. | n.d. | n.d. | n.d. |

**Table 2.** *Cont.*

| Wt.% | Baryte | Gypsum | | Jarosite | Alunite | Na-Rich Jarosite | K-Rich Natrojarosite | Natro-Alunite | Natrojarosite | |
|---|---|---|---|---|---|---|---|---|---|---|
| Location | Dachnoe | Donnoe | Dachnoe | | | Donnoe | | | Donnoe | Dachnoe |
| NH$_4$ | n.d. | n.d. | n.d. | n.d. | n.d. | n.d. | n.d. | 0.11 | 0.15 | 0.17 |
| Mg | 0.01 | n.d. | 0.00 | 0.02 | 0.00 | 0.01 | 0.02 | 0.01 | 0.02 | 0.05 |
| Co | n.d. | n.d. | n.d. | 0.01 | 0.00 | 0.01 | 0.02 | 0.01 | 0.02 | n.d. |
| Ni | n.d. | n.d. | n.d. | 0.01 | 0.00 | 0.01 | 0.02 | 0.00 | n.d. | n.d. |
| Ti | n.d. | n.d. | n.d. | n.d. | n.d. | 0.01 | n.d. | n.d. | 0.01 | 0.03 |
| Fe$^{2+}$ | n.d. | 0.01 | 0.01 | n.d. | n.d. | n.d. | n.d. | n.d. | n.d. | n.d. |
| Al | n.d. | n.d. | n.d. | 0.67 | 2.43 | 0.62 | 0.51 | 2.13 | 0.45 | 0.53 |
| Fe$^{3+}$ | n.d. | n.d. | n.d. | 2.28 | 0.57 | 2.35 | 2.44 | 0.86 | 2.49 | 2.39 |
| S | 1.04 | 1.03 | 1.00 | 2.11 | 1.90 | 2.08 | 2.06 | 2.00 | 2.01 | 2.02 |
| P | n.d. | n.d. | n.d. | 0.05 | 0.17 | 0.02 | 0.03 | 0.01 | 0.04 | 0.06 |
| H$_2$O | n.d. | 2.00 | 2.00 | n.d. | n.d. | n.d. | n.d. | n.d. | n.d. | n.d. |
| OH | n.d. | n.d. | n.d. | 6.00 | 6.00 | 6.00 | 6.00 | 6.00 | 6.00 | 6.00 |

Note: the oxidation state of iron corresponds to that in the ideal formula of the identified mineral. n—Number of analyses, n.d.—not detected. [1] the oxidation state of Fe is taken in agreement with ideal chemical formula; [2] H$_2$O/OH is taken as in ideal chemical formula; [3] the content of NH4 is calculated based on the charge balance.

**Table 3.** Chemical composition of amarillite and alum-group minerals: tschermigite, lonecreekite and alum-(Na) from Dachnoe thermal field normalized to 100%.

| Wt.% | Tschermigite | Lonecreekite | Alum-(Na) | Amarillite |
|---|---|---|---|---|
| *n* | 13 | 9 | 11 | 16 |
| Na$_2$O | n.d. | n.d. | 4.18 | 8.90 |
| MgO | n.d. | n.d. | 0.26 | 0.72 |
| Al$_2$O$_3$ | 10.48 | 0.37 | 9.80 | 2.07 |
| Fe$_2$O$_3$ [1] | 0.83 | 16.19 | 1.07 | 17.12 |
| SO$_3$ | 36.51 | 33.12 | 32.84 | 41.70 |
| P$_2$O$_5$ | n.d. | n.d. | 0.17 | 0.23 |
| H$_2$O [2] | 46.60 | 45.35 | 50.00 | 29.50 |
| (NH$_4$)$_2$O [3] | 5.58 | 4.99 | 1.70 | n.d. |
| **Total** | **100.00** | **100.00** | **100.00** | **100.00** |
| *apfu* calculated on the basis of Fe + Al + Mg = 1 | | | | |
| NH$_4$ | 0.99 | 0.91 | 0.31 | n.d. |
| Na | n.d. | n.d. | 0.64 | 1.05 |
| Mg | n.d. | n.d. | 0.03 | 0.07 |
| Al | 0.95 | 0.03 | 0.91 | 0.14 |
| Fe$^{3+}$ | 0.05 | 0.97 | 0.06 | 0.79 |
| S | 2.11 | 1.97 | 1.94 | 1.91 |
| P | n.d. | n.d. | 0.01 | 0.03 |
| H$_2$O | 12.00 | 12.00 | 12.00 | 6.00 |

*n*—Number of obtained analyses; n.d.—not detected. [1] the oxidation state of Fe is taken in agreement with ideal chemical formula; [2] H$_2$O/OH is taken as in ideal chemical formula; [3] the content of NH$_4$ is calculated based on the charge balance.

Gypsum is abundant in both fields (Donnoe and Dachnoe), its chemical composition (Tables 2 and 3, Figure 4) almost corresponds to the ideal chemical formula, $CaSO_4 \times 2H_2O$, and negligible Fe content up to 0.01 *apfu* may be present.
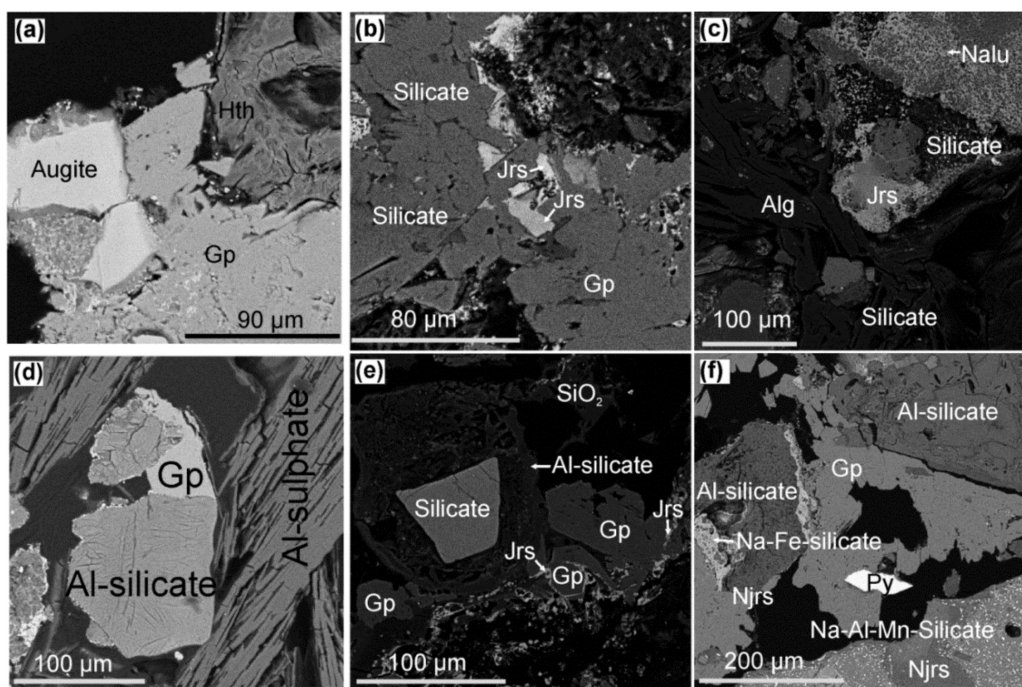


**Figure 4.** BSE images of efflorescent samples from Donnoe fumarole field: (**a**) halotrichite with gypsum, (**b**) jarosite with gypsum, (**c**) jarosite, natroalunite and alunogen, (**d**) gypsum with Al-silicate and Al-sulphate, (**e**) jarosite with gypsum and (**f**) natrojarosite with gypsum. Jrs—jarosite; Njrs—natrojarosite; Py—pyrite; Alg—alunogen; Gp—gypsum; Nalu—natroalunite, Hth—halotrichite.

In samples from the Dachnoe thermal field, we found three baryte grains with sizes of 30–40 × 20 μm. Trace amounts of Sr and Mg were found in the composition of baryte as 0.03 and 0.01 *apfu*, respectively (Table 2). Baryte was found in association with Al-sulphates identified as alunogen.

Within the alunite-supergroup, four minerals were found: alunite, jarosite, natroalunite, natrojarosite (Figure 4), and intermediate chemical varieties with Na/K ~1:1 and corresponding to Na-rich jarosite and K-rich natrojarosite (Table 2). All four detected alunite supergroup minerals were found at the Donnoe fumarole field, whereas at the Dachnoe thermal field only natrojarosite (Figure 5) hase been identified.

Jarosite and alunite have very similar Na/K ratios, being ~0.2/0.7 and 0.2/0.6, respectively. Jarosite is enriched by Ca (0.15 *apfu*), while alunite has Sr, Ca, and Ba impurities (0.07, 0.04 and 0.01 *apfu*, respectively). The potential mechanism of extra charge (produced by divalent cation in the *D* site) compensation is deprotonation of some OH groups and/or phosphorous (P) incorporation to sulphate tetrahedra. Natrojarosite and natroalunite also have similar Na/K ratios that are ~0.7/0.2 and 0.6/0.2, respectively. At the same time, divalent cations (Ca, Ba, and Sr) at the *D* site are nearly absent (only 0.04 *apfu* of Ca occurs in natroalunite) and the sum of *D* site cations is 0.83–0.89 *apfu*; this results in the deficit of positive charge (Table 2). Thus, we suppose that 0.11 (for natrojarosite) and 0.15/0.17 (for natroalunite) *apfu* of $(NH_4)^+$ cation occurs in the chemical composition of these minerals. Two varieties have the same content of K and Na that correspond to Na-rich jarosite with Na/K/Ca (*apfu*) = 0.49/0.50/0.01 and K-rich natrojarosite with Na/K/Ca = 0.49/0.47/0.04.
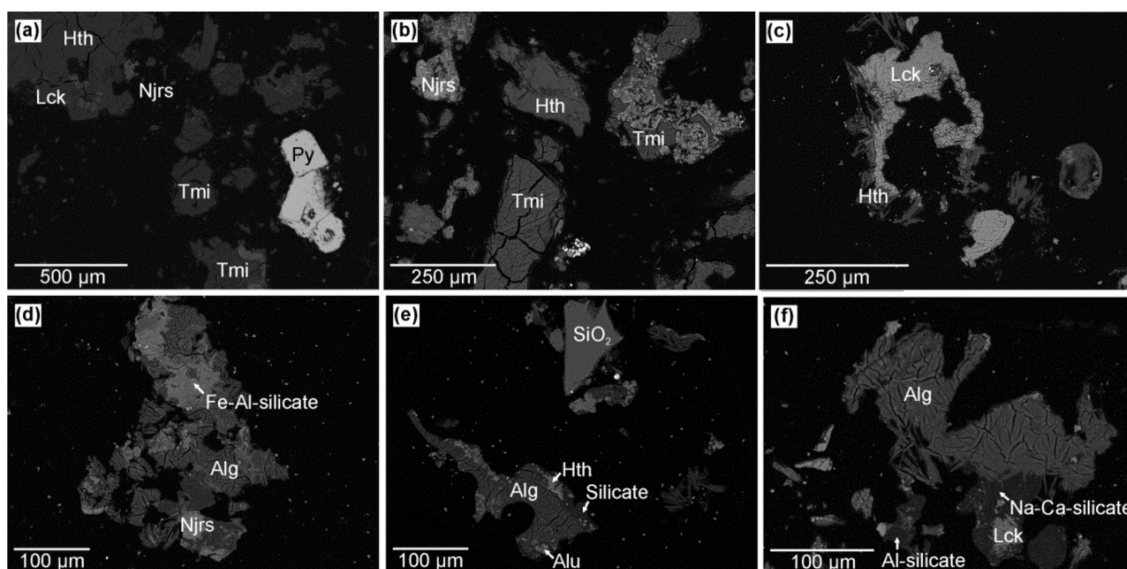
**Figure 5.** BSE images of efflorescent samples from Dachnoe thermal field: (**a**) alum-group minerals (tschermigite and lonecreekite), natrojarosite, halotrichite; (**b**) tschermigite, natrojarosite, halotrichite; (**c**) lonecreekite, halotrichite; (**d**) natrojarosite and alunogen; (**e**) alunite, alugonen and halotrichite; (**f**) lonecreekite with alunogen. Hth—halotrichite, Njrs—natrojarosite, Lck—lonecreekite, Py—pyrite, Tmi—tschermigite, Alg—alunogen, $SiO_2$—silica forms.

Even though both the $Fe^{3+}$- and Al-dominant alunite supergroup minerals were detected, the $Fe^{3+}$/Al ratios do not show wide variation in each of the minerals. For $Fe^{3+}$-dominant minerals, the highest $Fe^{3+}$/Al ratio is ~5:1, and the lowest is 3.4:1. For $Al^{3+}$-dominant minerals, the $Al/Fe^{3+}$ ratios are 4.3:1 and 2.5:1. All samples bear minor Mg impurity from 0.01 to 0.02 *apfu* for the Donnoe fumarole field and 0.05 *apfu* for the Dachnoe thermal field. Remarkably, alunite-group minerals from the Donnoe fumarole field bear small contents of Co and Ni in the amount of 0.01–0.02 *apfu* for each of the elements. Minor impurity of Ti up to 0.01 *apfu* occur in samples from the Donnoe fumarole field, while Ti in the sample from the Dachnoe thermal field is 0.03 *apfu*. The P impurity is present in all alunite supergroup minerals and its content varies from 0.01 to 0.17 *apfu* in samples from the Donnoe fumarole field and it is 0.06 *apfu* for samples from the Dachnoe thermal field.

At the Dachnoe thermal field, two Na-sulphates were found: amarillite and alum-Na (Figure 6). Since two ammonium minerals of the alum group: tschermigite and lonecreekite are found in association with the alum-(Na), their chemical composition is also given (Table 3).
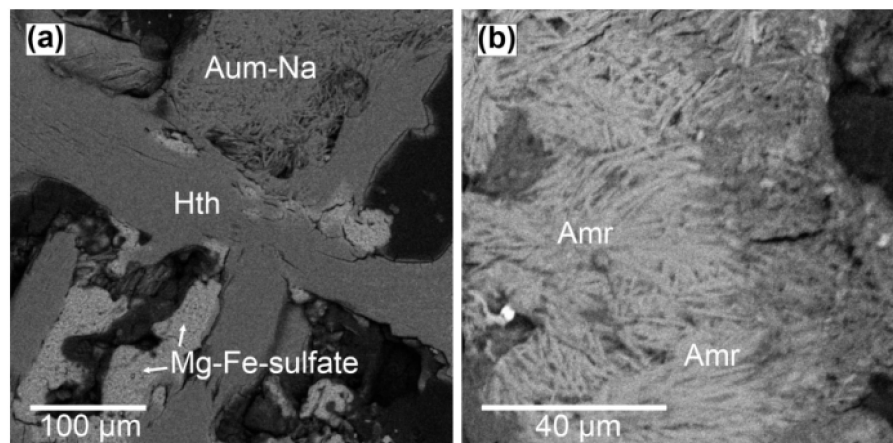


**Figure 6.** BSE images of (**a**) alum-(Na), (aum-Na), and (**b**) amarillite (Amr) from Dachnoe thermal field. Hth—halotrichite.

Amarillite is found in association with halotrichite and gypsum. The mineral has a rather well-defined stoichiometry Na/(Fe$^{3+}$ + Al + Mg)/(S + P) = 1.05/1.00/1.94 (Table 3). The mineral is P bearing (0.03 *apfu*) and contains Al and Mg (in Fe$^{3+}$-site) as 0.15 and 0.07 *apfu*, respectively.

Alum-(Na) is characterized by the presence of Na and NH$_4$ univalent cations in the ratio~2:1 (Table 3). The content of Al (0.91 *apfu*) strongly prevails over Fe (0.06 *apfu*) and Mg (0.03 *apfu*), the mineral contains 0.01 *apfu* of P. Tschermigite has a similar feature, with the strong predominance of Al (0.95 *apfu*) over Fe (0.05 *apfu*). However, solely NH$_4$ occurs as a monovalent cation. In lonecreekite, Fe$^{3+}$ (0.97 *apfu*) strongly prevails over Al (0.03 *apfu*). Only NH$_4$ occurs as a univalent cation and no substitution is observed for SO$_4$ tetrahedra, as for tschermigite.

### 3.3. Chemical Composition of Thermal Water

The thermal waters from the Dachnoe thermal field have been divided into 4 groups: water with pH < 3, pH in the range 3.5–4.7, pH > 6, and gas condensate of gas-steam vents (pH ~5). The main cations and anions of thermal water and their relative contents are given in Table S2. The relative content of the main cations represented by H, Na, K, NH$_4$, Ca, Mg, Fe$^{2+}$, Fe$^{3+}$ and Al in different proportions (Table S2) is shown as pie charts in Figure 7 with resemblance to the data on the chemical composition of thermal water from the Donnoe fumarole field reported previously [17]. The main anion is sulphate in thermal water and sulphate or bicarbonate in gas condensate (Table S2). The strongly dominant cation in the gas condensate is NH$_4$ in quantities subordinate to Ca and Mg (Figure 7).
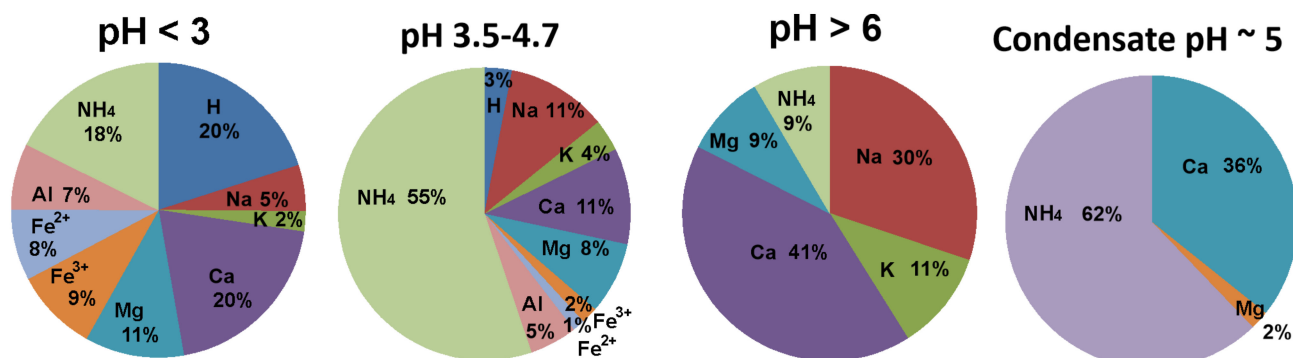


**Figure 7.** Fractional ratios of basic cations in thermal waters and gas-condensate from Dachnoe thermal field.

## 4. Discussion

### 4.1. Chemical Composition of Sulphate Efflorescent Minerals

From a mineralogical point of view, jarosite, alunite, natroalunite and natrojarosite belong to the alunite supergroup [34], which includes about 60 minerals. The general formula of alunite-supergroup minerals is represented as $DG_3(TX_4)_2X'_6$, where $D$ is a tetravalent, trivalent, divalent, or monovalent cation or a partial vacancy; $G$ is a trivalent cation and minor divalent cations; $T$ is a hexavalent, pentavalent cation and minor Si$^{4+}$; and $X/X'$ is O, (OH), minor F and possibly H$_2$O. The common constituents are $D$ = Na, K, Pb, Rb, NH$_4$, Ag, H$_3$O or H$_2$O; $G$ = Al, Fe$^{3+}$, V$^{3+}$ or Ga$^{3+}$; minor Cu, Zn, Ge; and $T$ = S, As, P [34,35]. The majority of alunite-supergroup minerals is isotypic and crystallize in $R−3m$ or $R3m$ space groups of the so-called alunite structure type. It has been shown by numerous previous studies, summarized in [36], that the alunite structure type shows outstanding flexibility in terms of incorporation of different size and charge cations that has even been referred to as a "garbage-can" structure.

The alunite-supergroup minerals show wide variation in Na/K ratio, resulting in the formation of both Na-dominant (natroalunite and natrojarosite) and K-dominant (jarosite and alunite) varieties. Interestingly, two chemical varieties of alunite supergroup minerals

with Na/K ~1:1 were found. A wide variation of Na/K ratios are observed for samples from the Donnoe fumarole field, whereas at the Dachnoe thermal field only (K-depleted) natrojarosite was found. Jarosite and alunite are enriched by divalent *A*-site cations, Ba and Sr, while natrojarosite and natroalunite are enriched by the $(NH_4)^+$ cation (Table 3). There is clear compositional segregation between Al- and $Fe^{3+}$-minerals, so the $Fe^{3+}$ content in the Al-dominated *D* site does not exceed 1/4, while the highest $Fe^{3+}$ content in the Al site is 1/6. In the experimental study of volcanic rocks from Chile and Argentina [37], it was shown that factors responsible for Na/K variation in alunite-group minerals are temperature (a significant difference occurs above 100 °C, which was not the subject of the studied localities) and Na concentrations in the source fluid. The latter depends on the composition of host rocks: higher Na concentrations are observed when andesite is leached, while K-varieties are confined to rocks with a composition from dacitic to granitic.

The thermal waters and pore solutions from the Donnoe fumarole field have varying Na/K ratios; in the same type of water, both K and Na can dominate at different sampling points [18]. In all types of water collected from the Dachnoe thermal field (Figure 7) the Na concentration is 2–3 times higher than that of K. The higher content of K at the Donnoe fumarole field may be explained by the presence of rhyodacite series among the host rocks. The wide variation of the Na/K ratio in the samples from the Donnoe fumarole field reflects the complexity of the crystallization process, which is associated with the constantly changing (locally) composition of pore solutions and physicochemical parameters, which, in particular, are sensitive to weather conditions such as the level and frequency of precipitation, temperature, and humidity. Based on data from the literature [38,39], we also suppose that the formation of alunite-group minerals at the Mutnovsky volcano is determined by very local pH parameters of the pore solution: $Fe^{3+}$-members (jarosite and natrojarosite) crystallize at lower pH in comparison to $Al^{3+}$-species (alunite and natroalunite). Alunite-supergroup minerals are commonly found in intimate association with primary silicates, and they replace them (Figure 4) [38,40]. The residue obtained from the alteration of silicates minerals leads to the formation of silicate dioxide minerals: opal, cristobalite, and tridymite. The jarosite rim around shaped gypsum crystal (Figure 4) reflects jarosite formation after gypsum.

The general formula of alum-group minerals can be expressed as $AM^{3+}(SO_4)_2 \times 12H_2O$, where *A*—monovalent cation; *M*—trivalent cation. The *A*-site is represented by Na and $(NH_4)^+$ in alum-(Na) with $Na/NH_4 = 2:1$ and solely by $(NH_4)^+$ cation in tschermigite and lonecreekite. There is clear compositional segregation between Al and $Fe^{3+}$ cations: tschermigite and alum-(Na) are Al-dominant with Fe content about 10%, while lonecreekite is Fe-dominant with Al content < 6%. Ammonium minerals differ from others in that they do not contain either Na or P. It is of interest to note that the chemical formula of tschermigite from the Nizhny-Koshelevsky thermal field (associated with Koshelevsky volcano, Kamchatka, Russia) almost corresponds to the ideal; the mineral has a minor content of K (0.02 *apfu*) and Na (0.02 *apfu*) in the $(NH_4)^+$-dominant *A* site and the $M^{3+}$ cation is represented exclusively by Al [41]. Alum-group minerals show very limited $Fe^{3+}$ content in Al-dominant members and *vice versa*; the anion is represented almost exclusively by $SO_4$ and the isomorphism of monovalent cation is observed only for Na-dominant members. The crystallization of ammonium minerals occurs either near ammonia-emitting low-temperature gas-steam vents (<100 °C) where tschermigite is found in or near fumaroles (100–150 °C) around which mascagnite and letovicite are observed. The source of nitrogen has not yet been determined.

Taking into account the chemical composition (Tables 2 and 3) of $Fe^{3+}$- and Al-sulphates and the existence of alunite with jarosite and tschermigite with lonecreekite at the microscale (Figure 5a), we suggest that the presence of Al and $Fe^{3+}$ at the fumarole and thermal fields of the Mutnovsky volcano leads to the formation of different minerals either $Fe^{3+}$- or Al-dominant rather than a complete series of solid solutions. Similar suggestions on the compositional segregation of $Fe^{3+}$- and Al in alunite supergroup members have been observed previously for samples from Broken Hill (New South Wales, Australia) [42],

while a large compositional gap between alunite-natroalunite and jarosite-natrojarosite in terms of Na/K ratio has been shown in samples from Goldfield, Nevada (USA) and explained as features of the crystallization process [40].

Amarillite has the following chemical formula: $Na_{1.05}(Fe^{3+}_{0.79}Al_{0.14}Mg_{0.07})_{\Sigma 1.00}[(S_{0.955}P_{0.015})O_4]_2 \times 6H_2O$. Amarillite does not show the substitution of Na by other monovalent cations; however, Al and Mg are found in addition to $Fe^{3+}$ and some P substitutes for S. Amarillite is a rare mineral that, in the majority of cases, occurs as a sulphide-oxidation product. However, findings of this mineral, where its formation is associated with volcanic activity, are also known. The mineral has been described at the solfataric field at Campi Flegrei, Italy [43] and in fumaroles of the Tolbachik volcano (Kamchatka, Russia) [44].

Only one Ca sulphate has been identified that is abundant at both the Donnoe fumarole field and Dachnoe thermal field—gypsum. Gypsum has a very persistent chemical composition that does not reflect a difference in the conditions of its formation, which is consistent with existing observations [45]. In general, gypsum is a common mineral of low-temperature volcanic environments since the main dehydration of gypsum occurs above 95 °C [46]. The presence of gypsum in a medium-temperature fumarole in association with mascagnite (Figure 3) indicates the possibility that the sample originally was partially dehydrated. It has been recently shown that the morphology of terrestrial gypsum from hot springs (such as the example of Uzon Kaldera, Kamchatka, Russia) is, to some extent, shaped by the microbial community that is widespread at thermal fields [47]. Thus, in accord with [47], SEM images of gypsum from volcanic environments may serve as a reference for the detection of microbial life on Mars. It is worth noting that gypsum can form in slightly different conditions at thermal fields: as surface efflorescent, well-formed crystals in argillic strata, and massive deposits [48]. In the case of efflorescent, gypsum is found as shapeless masses or fine-grained precipitate.

Baryte occurs as a very minor phase at the Dachnoe thermal field and it plays the role of a Sr concentrator. Regarding volcanic settings, baryte is described at various low-temperature environments (thermal fields) and in medium- and high-temperature fumaroles [49,50]. The enrichment of thermal water by Ba and Sr simultaneously may be due to seawater entering the deep geothermal reservoir, which agrees with [51]; however, this requires more detailed study.

### *4.2. Mineral-Forming Chemical Elements*

The reported suite of surface efflorescent minerals herein is produced by fluid/rock interaction and appears to be the last stage of mineral formation. These phases are in constant dynamics and undergo numerous circles of recrystallization due to high variability in the location of thermal manifestations and the impact of atmospheric precipitation. The (volcanic) steam bears such main (mineral-forming) chemical elements as N ($NH_4$), Ca, minor Mg, S, O, and H (Table S2) and has a pH of ~5. Oxidation of the discharging fluid occurs on the day surface, so the thermal water from the fields is more acidic with a pH below 3 in most cases (Table S2), and it is enriched by elements such as Na, K, Fe, and Al that, as in the literature [52–54], are supposed to come from the leaching of the host rocks. It is interesting that the main elements in the chemical composition of minerals fully correspond to the main elements of thermal water (Tables 1–3, Figure 7). The high concentration of $NH_4$ is characteristic of pore solution near fumaroles. Ammonium sulphates of the Dachnoe thermal field are highly hydrated and represented by alums (tschermigite and lonecreekite), while at the Donnoe fumarole field, they are represented by anhydrous species letovicite and mascagnite, indicating the higher temperature formation (deposited around fumarole with temperature ~120–150 °C) of the latter paragenesis. The composition of the thermal water at each sampling point is unique, as it is determined by the proportion of the volcanic component, meteor water, pH, temperature, precipitation, surrounding rocks, and other parameters. Variations in these parameters lead to the formation of different mineral associations: ATM-alunogen-$SiO_2$, alum-gypsum-alunogen/halotrichite-$SiO_2$, mascagnite-gypsum, letovicite-kaolinite-tridymite, and alum-voltaite-alunogen [55]

(where ATM—alunite-type minerals; alum—alum-group minerals; and $SiO_2$—silica dioxide minerals as opal, cristobalite, and tridymite). Taking into account the variability of the environment and the conditions of crystallization, it is practically impossible to trace the relationship between the mineral association and certain parameters. To solve such a problem, it is necessary to carry out a large number of model experiments on the influence of various parameters on phase formation.

Of particular interest is the analysis of impurity elements in minerals of the alunite group. The presence of Ca, Ba, Sr, and $NH_4$ in Na and K sites; Mg, Co, Ni, and Ti in Al and $Fe^{3+}$ sites; and P in the S site agrees with the crystal chemistry of alunite-supergroup minerals [36]. At the same time, chemical elements such as Co, Ni, and Ti look the most exotic. Previously, it was shown [18] that the thermal waters of the Mutnovsky volcano are unique due to the high content of trace elements such as Ti, V, Cr, Co, and Ni, and their concentration is several times higher than at other volcanos such as Etna (Sicily, Italy), Vulcano (Aeolian Islands, Italy), El Chichon (Chiapas, Mexico), and Ebeko (Kuril islands, Russia). It has been suggested [18] that these chemical elements come from deep and uncommon sources and that they should not concentrate in the surface minerals. Our study shows the opposite; that Ti, Co, and Ni concentrate as impurities (as tenths of wt.%) in the alunite-group minerals found at the field's surface. It is noteworthy that the high concentration of Ppresents in all types of waters from the Mutnovsky volcano [18], and the highest concentration of P was found at the Donnoe fumarole field [18] that is in a good correlation with chemical analyses obtained for sulphates.

### 4.3. Implication of Efflorescent Sulphates for Volcanology and Planetary Science

Considering the main elements, the geochemical specificity lies in the presence of ammonia brought by steam and the precipitation of ammonium minerals. Of course, the discovery of ammonium minerals on Mars or other planets would be a big step, but such phases have not yet been reliably recorded. The rest of the cations, Na, K, Ca, and Ba, are likely delivered from the host rocks via leaching. This process of hydrothermal alteration by acidic solution is common for volcanic settings and artificially produced acid-mine drainage (AMD) systems [56]. The Ca sulphate is represented by gypsum, which is a very common mineral and does not show the more or less significant substitution of the Ca cation. Baryte is found in various environments; regarding volcanic systems, it tends to be found at a low-temperature. The Sr impurity in baryte is not a rarity and is more characteristic of environments where seawater has evaporated and produced baryte [57]. The K-Na alunite-type minerals (alunite, jarosite, natroalunite, and natrojarosite) are common in volcanic environments and AMD systems. The samples from the Donnoe fumarole field show that samples with different K/Na and/or Fe/Al ratios can be found in close association. This indicates that structurally similar phases with different ratios of K/Na and/or Fe/Al (referring to different mineral species) can precipitate from the same solution, probably as a result of the complex crystallization process when one mineral leads to a change in the composition of the solution and its physicochemical parameters triggering subsequent crystallization of other phases. Thus, in certain conditions, instead of obtaining one mineral of the alunite group, which could subsequently be used as a reference to specific environments, we obtain 2–4 similar minerals with different K/Na and Fe/Al ratios and even intermediate forms with K/Na ~1:1. It is unlikely that we can fully use the composition of such a complex system for a direct comparison with other terrestrial and extraterrestrial environments.

However, if we consider the specifics of the Mutnovsky volcano thermal waters in terms of trace elements, we will find that it is enriched by Co, Ni, Ti, and P [18]. The impurity of these elements is found in the surface efflorescent, in particular, in alunite-group minerals that have structural flexibility for uptake of different sizes and charge cations to the crystal structure [36]. Thus, the trace-element composition of alunite-group minerals can be considered as typomorphic to volcanic thermal waters of Mutnovsky volcano. The ability to capture and concentrate elements by alunite-type minerals from aqueous solutions is well

known and even served as the basis for proposals for the use of jarosite and natroalunite for removal of heavy metals from aqueous solutions [40,58] and divalent alunite-group minerals as a host for radionuclides [58]. These phases have also been considered as matrices for the uptake of heavy metals in AMD systems, which can limit the environmental impact [58]. Although these phases are known and widely described in altered volcanic rocks in the process of hydrothermal or fumarolic activity [58–62], features of their chemical composition relative to thermal water or specification of typomorphic features have not previously been carried out, to the best of our knowledge. Thus, minerals of the alunite group formed under these conditions can carry information about the chemical composition of the contacting medium. In this case, the chemical analysis of alunite-group minerals can be used as a tool to reconstruct the conditions of mineral formation in the volcanic and paleovolcanic (fossil) settings of Earth, Mars, and other objects in the Solar system. The potential use of alunite-supergroup minerals is enhanced by their extraordinary stability over a wide range of pH values (from 1 to 10) and at temperatures at least from $-140$ (characteristic for Mars) up to 400 °C (characteristic for volcanic settings) [36,40]. As the detailed chemical examination of Martian rocks (either returned or in situ) shortly becomes possible, the terrestrial hot spring efflorescent sulphates, which carry information on specific geological environments that are influenced by hydrothermal activity, can be used as references for mineral assemblages, the chemical composition of minerals in terms of main and trace elements for the reconstruction of Martian geology, and possible volcanic activity. At the same time, paleohydrothermal and paleofumarole systems are frequent in areas of active volcanism. They may have varying degrees of alteration, but they contain clay minerals, minerals of the alunite group. Often, when studying such systems, it becomes necessary to obtain information about circulation in the past hydrothermal solution and its similarity with modern solutions. Our study shows that minerals of the alunite group are potentially informative phases for establishing the chemical features of such systems.

## 5. Conclusions

We have described modern efflorescent mineralogy of active low-temperature geothermal fields, including ammonia-emitting fumarole, which have an unusual assemblage of sulphate minerals. The most abundant minerals are sulphates of Fe-Al, Al, and Ca: halotrichite, alunogen, and gypsum. In addition, sulphates of alkaline and alkaline earth cations, Na, K, Ba, and $NH_4$, are widespread but form crystals and precipitates of a smaller size. These are alunite-jarosite quadrilateral defined by alunite, natroalunite, jarosite, and natrojarosite: alum-group minerals, such as tschermigite, lonecrekite, and alum-Na; amarillite; baryte; letovicite and mascagnite. The discovered mineral associations are unique and characteristic of low-temperature geothermal fields and fumaroles, where mineral formation is a low-temperature process in an acidic environment. The broadest ability for isomorphism among the identified minerals is observed for alunite-supergroup minerals that contain Ca, Ba, Sr, and $NH_4$ in addition to Na and K as well as Mg, Co, Ni, Ti in addition to Al and Fe, while P substitutes for S. The presence of Ni, Co, Ti, P, and $NH_4$ impurities in the composition of alunite-supergroup minerals reflects the unique composition of the thermal water of the Mutnovsky volcano. Taking into account the crystal-chemical variability and good chemical resistance of alunite-group minerals, they can be considered as indicators of the geochemistry of the medium leading to the alteration of volcanic rocks. In this case, the detailed chemical analyses of alunite-supergroup minerals may help to reconstruct geochemical conditions in ancient hydrothermal systems.

**Supplementary Materials:** The following are available online at https://www.mdpi.com/article/10.3390/min12050600/s1, Table S1: The powder X-ray diffraction data for samples shown in Figure 3 and Table S2: The chemical composition of the thermal water and gas-condensate from the Dachnoe thermal field.

## References

1. Varekamp, J.C.; Ouimette, A.P.; Herman, S.W.; Flynn, K.S.; Bermudez, A.; Delpino, D. Naturally acid waters from Copahue volcano, Argentina. *Appl. Geochem.* **2009**, *24*, 208–220. [CrossRef]

2. Henley, R.W. Hyperacidic volcanic lakes, metal sinks and magmatic gas expansion in arc volcanoes. In *Volcanic Lake*; Rouwet, D., Christenson, B.W., Tassi, F., Vandemeulebrouck, J., Eds.; Springer: Berlin/Heidelberg, Germany, 2015; pp. 155–178. [CrossRef]

3. Inguaggiato, C.; García, M.Á.P.; Maldonado, L.F.M.; Peiffer, L.; Pappaterra, S.; Brusca, L. Precipitation of secondary minerals in acid sulphate-chloride waters traced by major, minor and rare earth elements in waters: The case of Puracé volcano (Colombia). *J. Volcanol. Geotherm. Res.* **2020**, *407*, 107106. [CrossRef]

4. Adams, P.M.; Lynch, D.K.; Buckland, K.N.; Johnson, P.D.; Tratt, D.M. Sulfate mineralogy of fumaroles in the Salton Sea Geothermal Field, Imperial County, California. *J. Volcanol. Geotherm. Res.* **2017**, *347*, 15–43. [CrossRef]

5. McHenry, L.J.; Carson, G.L.; Dixon, D.T.; Vickery, C.L. Secondary minerals associated with Lassen fumaroles and hot springs: Implications for martian hydrothermal deposits. *Am. Mineral.* **2017**, *102*, 1418–1434. [CrossRef]

6. McCollom, T.M.; Hynek, B.M.; Rogers, K.; Moskowitz, B.; Berquó, T.S. Chemical and mineralogical trends during acid-sulfate alteration of pyroclastic basalt at Cerro Negro volcano and implications for early Mars. *J. Geophys. Res. Planets* **2013**, *118*, 1719–1751. [CrossRef]

7. Ciesielczuk, J.; Żaba, J.; Bzowska, G.; Gaidzik, K.; Głogowska, M. Sulphate efflorescences at the geyser near Pinchollo, southern Peru. *J. S. Am. Earth Sci.* **2013**, *42*, 186–193. [CrossRef]

8. Rodríguez, A.; Van Bergen, M.J. Volcanic hydrothermal systems as potential analogues of Martian sulphate-rich terrains. *Neth. J. Geosci.* **2016**, *99*, 153–169. [CrossRef]

9. Klingelhöfer, G.; Morris, R.V.; Bernhardt, B.; Schröder, C.; Rodionov, D.S.; De Souza, P.A.; Yen, A.; Gellert, R.; Evlanov, E.N.; Zubkov, B.; et al. Jarosite and hematite at Meridiani Planum from Opportunity's Mössbauer spectrometer. *Science* **2004**, *306*, 1740–1745. [CrossRef]

10. Morris, R.V.; Squyres, S.; Arvidson, R.E.; Bell, J.F., III; Christensen, P.C.; Gorevan, S.; Herkenhoff, K.; Klingelhöfer, G.; Rieder, R.; Farrand, W.; et al. A first look at the mineralogy and geochemistry of the MER-B landing site in Meridiani Planum. In Proceedings of the 35th Lunar and Planetary Science Conference, League City, TX, USA, 15–19 March 2004. Abstract No. 2179.

11. Farrand, W.H.; Glotch, T.D.; Rice, J.W., Jr.; Hurowitz, J.A.; Swayze, G.A. Discovery of jarosite within the Mawrth Vallis region of Mars: Implications for the geologic history of the region. *Icarus* **2009**, *204*, 478–488. [CrossRef]

12. Madden, M.E.E.; Bodnar, R.J.; Rimstidt, J.D. Jarosite as an indicator of water-limited chemical weathering on Mars. *Nature* **2004**, *431*, 821–823. [CrossRef]

13. Navrotsky, A.; Forray, F.L.; Drouet, C. Jarosite stability on Mars. *Icarus* **2005**, *176*, 250–253. [CrossRef]

14. Mills, S.J.; Nestola, F.; Kahlenberg, V.; Christy, A.G.; Hejny, C.; Redhammer, G.J. Looking for jarosite on Mars: The low-temperature crystal structure of jarosite. *Am. Mineral.* **2013**, *98*, 1966–1971. [CrossRef]

15. Bishop, J.L.; Murad, E. The visible and infrared spectral properties of jarosite and alunite. *Am. Mineral.* **2005**, *90*, 1100–1107. [CrossRef]

16. Sergeeva, A.V. Infrared Spectra of Alunite-Group Minerals Formed on Thermal Fields. *J. Appl. Spectrosc.* **2019**, *86*, 371–378. [CrossRef]

17. McCollom, T.M.; Ehlmann, B.L.; Wang, A.; Hynek, B.M.; Moskowitz, B.; Berquó, T.S. Detection of iron substitution in natroalunite-natrojarosite solid solutions and potential implications for Mars. *Am. Mineral.* **2014**, *99*, 948–964. [CrossRef]

18. Bortnikova, S.B.; Gavrilenko, G.M.; Bessonova, E.P.; Lapuchov, A.S. The hydrogeochemistry of thermal springs on Mutnovskii Volcano, southern Kamchatka. *J. Volcanol. Seismol.* **2009**, *3*, 388–404. [CrossRef]

19. Košek, F.; Culka, A.; Fornasini, L.; Vandenabeele, P.; Rousaki, A.; Mirao, J.; Bersani, D.; Candeias, A.; Jehlička, J. Application of a handheld Raman spectrometer for the screening of colored secondary sulfates in abandoned mining areas—The case of the São Domingos Mine (Iberian Pyrite Belt). *J. Raman Spectrosc.* **2020**, *51*, 1186–1199. [CrossRef]

20. Rull, F.; Guerrero, J.; Venegas, G.; Gázquel, F.; Medina, J. Spectroscopic Raman study of sulphate precipitation sequence in Rio Tinto mining district (SW Spain). *Environ. Sci. Pollut. Res. Int.* **2014**, *21*, 6783–6792. [CrossRef]

21. Žáček, V.; Škoda, R.; Laufek, F.; Ek, F.K.; Jehlička, J. Complementing knowledge about rare sulphates lonecreekite, $NH_4Fe^{3+}(SO_4)_2 \cdot 12H_2O$ and sabieite, $NH_4Fe^{3+}(SO_4)_2$: Chemical composition, XRD and RAMAN spectroscopy (Libušín near Kladno, the Czech Republic). *J. Geosci.* **2019**, *64*, 149–159. [CrossRef]

22. Košek, F.; Edwards, H.G.M.; Jehlička, J. Raman spectroscopic vibrational analysis of the complex iron sulfates clairite, metavoltine, and voltaite from the burning coal dump Anna I, Alsdorf, Germany. *J. Raman Spectrosc.* **2019**, *51*, 1454–1461. [CrossRef]

23. Vakin, E.A.; Pilipenko, G.F. Mutnovsky geothermal area. In *Kamchatka in Exploration and Use of Geothermal Resources in Volcanic Areas*, 1st ed.; Aladiyev, I.T., Sugrobov, V.M., Eds.; Nauka: Moscow, Russia, 1979; pp. 36–45. (In Russian)

24. Vakin, E.A.; Kirsanov, I.T.; Pronin, A.A. Active funnel of Mutnovsky volcano. In *Bulletin of the Kamchatka Volcanological Stations*, 1st ed.; Gushchenko, I.I., Ed.; Nauka: Moscow, Russia, 1966; Volume 40, pp. 25–35. (In Russian)

25. Serafimova, E.K. Features of the chemical composition of fumarole gases of Mutnovsky volcano. In *Bulletin of the Kamchatka Volcanological Stations*, 1st ed.; Gushchenko, I.I., Ed.; Nauka: Moscow, Russia, 1966; Volume 42, pp. 56–65. (In Russian)

26. Zelensky, M.E. Transport of Elements and Minersl Forming Conditions at High-Temperature Gas Dischargees from Mutnovsky Volcano (Kamchatka). Ph.D. Thesis, Institute of Volcanology, Petropavlovsk-Kamchatsky, Russia, 2003. (In Russian).

27. Kiryukhin, A.V.; Tranbenkova, A.G.; Bortnikova, S.B.; Fazlullin, S.M. Gas and Chemical Monitoring of the Mutnovsky (Dachny) Geothermal Field Exploration (Kamchatka, Russia). In Proceedings of the World Geothermal Congress, Antalya, Turkey, 24–29 April 2005.

28. Selyangin, O.B. Structure, substance and subsurface magma chambers of the volcanoes Mutnovsky and Gorely (Mutnovsky geothermal area, Kamchatka). I. geological position of the volcanoes). *GIAB №11, «Kamchatka-3»* **2016**, *31*, 365–400. (In Russian)

29. Bortnikova, S.B.; Sharapov, V.N.; Bessonova, E.P. Hydrothermal Composition of Springs at the Donnoe Fumarole Field, Mutnovsky Volcano (Southern Kamchatka) and Problems of Their Relation with Supercritical Magmatic Fluids. *Dokl. Earth Sci.* **2007**, *3*, 410–414. [CrossRef]

30. Leonov, V.L. *Structural Conditions of High-Temperature Fluids' Localization*, 1st ed.; Nauka: Moscow, Russia, 1989; p. 104. (In Russian)

31. Slyadnev, B.I.; Shapovalenko, V.N.; Krikun, N.F. *State Geological Map of the Russian Federation, Scale 1:1,000,000 (Third Generation). Series Koryaksko-Kurilskaya. Sheet N-57-Petropavlovsk-Kamchatsky*; VSEGEI: St. Petersburg, FL, USA, 2006.

32. Britvin, S.N.; Dolivo-Dobrovolsky, D.V.; Krzhizhanovskaya, M.G. Software for processing of X-ray powder diraction data obtained from the curved image plate detector of Rigaku RAXIS Rapid II diractometer. *Zap. Ross. Mineral. Obs.* **2017**, *146*, 104–107, (In Russian with English Abs.).

33. Balić-Žunić, T.; Garavelli, A.; Jakobsson, S.P.; Jonasson, K.; Katerinopoulos, A.; Kyriakopoulos, K.; Acquafredda, P. Fumarolic Minerals: An Overview of Active European Volcanoes. In *Updates in Volcanology, from Volcano Modelling to Volcano Geology*; Nemeth, K., Ed.; InTech: Rijeka, Croatia, 2016; pp. 267–322. [CrossRef]

34. Bayliss, P.; Kolitsch, U.; Nickel, E.H.; Pring, A. Alunite supergroup: Recommended nomenclature. *Mineral. Mag.* **2010**, *74*, 919–927. [CrossRef]

35. Stoffregen, R.E.; Alpers, C.N.; Jambor, J.L. Alunite-jarosite crystallography, thermodynamics, and geochronology. *Rev. Mineral. Geochem.* **2000**, *40*, 453–479. [CrossRef]

36. Kolitsch, U.; Pring, A. Crystal chemistry of the crandallite, beudantite and alunite groups: A review and evaluation of the suitability as storage materials for toxic metals. *J. Mineral. Petrol. Sci.* **2001**, *96*, 67–78. [CrossRef]

37. Deyell, C.L.; Dipple, G.M. Equilibrium mineral-fluid calculations and their application to the solid solution between alunite and natroalunite in the El Indio–Pascua belt of Chile and Argentina. *Chem. Geol.* **2005**, *215*, 219–234. [CrossRef]

38. Hladky, G.; Slansky, E. Stability of alunite minerals in aqueous solutions at normal temperature and pressure. *Bull. Mineral.* **1981**, *104*, 468–477. [CrossRef]

39. Sergeeva, A.V.; Zhitova, E.S.; Nuzhdaev, A.A.; Nazarova, M.A. Modeling the Mineral Formation Process on Thermoanomalies with Ammonium-Sulphate Thermal Waters: The Role of Acidity (pH). *J. Volcanol. Seismol.* **2022**, *1*, 29–53.

40. Papike, J.J.; Karner, J.M.; Spilde, M.N.; Shearer, C.K. Terrestrial analogs of martian sulfates: Major and minor element systematics of alunite-jarosite from Goldfield, Nevada. *Am. Mineral.* **2006**, *91*, 1197–1200. [CrossRef]

41. Zhitova, E.S.; Sergeeva, A.V.; Nuzhdaev, A.A.; Krzhizhanovskaya, M.G.; Chubarov, V.M. Tschermigite from thermal fields of Southern Kamchatka: High-temperature transformation and peculiarities of IR-spectrum. *Zap. Ross. Mineral. Obs.* **2019**, *148*, 100–116. (In Russian)

42. Rattray, K.J.; Taylor, M.R.; Bevan, D.J.M.; Pring, A. Compositional segregation and solid solution in the lead-dominant alunite-type minerals from Broken Hill, NSW. *Mineral. Mag.* **1996**, *60*, 779–785. [CrossRef]

43. Piochi, M.; Mormone, A.; Balassone, G.; Strauss, H.; Troise, C.; De Natale, G. Native sulfur, sulfates and sulfides from the active Campi Flegrei volcano (southern Italy): Genetic environments and degassing dynamics revealed by mineralogy and isotope geochemistry. *J. Volcanol. Geotherm. Res.* **2015**, *304*, 180–193. [CrossRef]

44. Pekov, I.V.; Koshlyakova, N.N.; Agakhanov, A.A.; Zubkova, N.V.; Belakovskiy, D.I.; Vigasina, M.F.; Turchkova, A.G.; Sidorov, E.G.; Pushcharovsky, D.Y. New arsenate minerals from the Arsenatnaya fumarole, Tolbachik volcano, Kamchatka, Russia. XV. Calciojohillerite, $NaCaMgMg_2(AsO_4)_3$, a member of the alluaudite group. *Mineral. Mag.* **2021**, *85*, 215–223. [CrossRef]

45. Africano, F.; Bernard, A. Acid alteration in the fumarolic environment of Usu volcano, Hokkaido, Japan. *J. Volcanol. Geotherm. Res.* **2000**, *97*, 475–495. [CrossRef]

46. Deer, W.A.; Howie, R.A.; Zussman, J. An Introduction to the Rock-Forming Minerals. *Mineral. Mag.* **1992**, *56*, 617–619. [CrossRef]

47. Tang, M.; Ehreiser, A.; Li, Y.L. Gypsum in modern Kamchatka volcanic hot springs and the Lower Cambrian black shale: Applied to the microbial-mediated precipitation of sulfates on Mars. *Am. Mineral.* **2014**, *99*, 2126–2137. [CrossRef]

48. Van Hinsberg, V.J.; Berlo, K.; Pinti, D.L.; Ghaleb, B. Gypsum precipitating from volcanic effluent as an archive of volcanic activity. *Front. Earth Sci.* **2021**, *9*, 764087. [CrossRef]

49. Inostroza, M.; Aguilera, F.; Menzies, A.; Layana, S.; González, C.; Ureta, G.; Sepulveda, J.; Sheller, S.; Böehm, S.; Barraza, M.; et al. Deposition of metals and metalloids in the fumarolic fields of Guallatiri and Lastarria volcanoes, northern Chile. *J. Volcanol. Geotherm. Res.* **2020**, *393*, 106803. [CrossRef]

50. Pekov, I.V.; Kovrugin, V.M.; Siidra, O.I.; Chukanov, N.V.; Belakovskiy, D.I.; Koshlyakova, N.N.; Yapaskurt, V.O.; Turchkova, A.G.; Möhn, G. Antofagastaite, $Na_2Ca(SO_4)_2 \cdot 1.5H2O$, a new mineral related to syngenite. *Mineral. Mag.* **2019**, *83*, 781–790. [CrossRef]

51. Zelenski, M.; Taran, Y. Geochemistry of volcanic and hydrothermal gases of Mutnovsky volcano, Kamchatka: Evidence for mantle, slab and atmosphere contributions to fluids of a typical arc volcano. *Bull. Volcanol.* **2011**, *73*, 373–394. [CrossRef]

52. Inioue, A.; Utada, M. Hydrothermal Alteration in the Kamikita Kuroko Mineralization Area. *Min. Geol.* **1991**, *41*, 203–218. [CrossRef]

53. Martin, R.; Rodgers, K.A.; Browne, P.R.L. The nature and significance of sulphate-rich, aluminous efflorescences from the Te Kopia geothermal field, Taupo Volcanic Zone, New Zealand. *Mineral. Mag.* **1999**, *63*, 413–419. [CrossRef]

54. Zhitova, E.S.; Siidra, O.I.; Belakovsky, D.I.; Shilovskikh, V.V.; Nuzhdaev, A.A.; Ismagilova, R.M. Ammoniovoltaite, $(NH_4)_2Fe^{2+}{}_5Fe^{3+}{}_3Al(SO_4)_{12}(H_2O)_{18}$, a new mineral from the Severo-Kambalny geothermal field, Kamchatka, Russia. *Mineral. Mag.* **2018**, *82*, 1057–1077. [CrossRef]

55. Carbone, C.; Dinelli, E.; Marescotti, P.; Gasparotto, G.; Lucchetti, G. The role of AMD secondary minerals in controlling environmental pollution: Indications from bulk leaching tests. *J. Geochem. Explor.* **2013**, *132*, 188–200. [CrossRef]

56. Hein, J.R.; Zierenberg, R.A.; Maynard, J.B.; Hannington, M.D. Barite-forming environments along a rifted continental margin, Southern California Borderland. *Deep-Sea Res. Part II* **2007**, *54*, 1327–1349. [CrossRef]

57. Luo, Z.; Mu, W.; Zhou, X.; Chen, Z. Removal and immobilization of arsenic from wastewater via arsenonatroalunite formation. *Environ. Technol.* **2021**, *42*, 1–10. [CrossRef]

58. Hudson-Edwards, K.A. Uptake and release of arsenic and antimony in alunite-jarosite and beudantite group minerals. *Am. Mineral.* **2019**, *104*, 633–640. [CrossRef]

59. Owen, N.D.; Cook, N.J.; Rollog, M.; Ehrig, K.J.; Schmandt, D.S.; Ram, R.; Brugger, J.; Ciobanu, C.L.; Wade, B.; Guagliardo, P. REE-, Sr-, Ca-aluminum-phosphate-sulfate minerals of the alunite supergroup and their role as hosts for radionuclides. *Am. Mineral.* **2019**, *104*, 1806–1819. [CrossRef]

60. Graham, I.J.; Robinson, B.W. Natroalunite on Ruapehu volcano, New Zealand. *Geochem. J.* **1986**, *20*, 249–253. [CrossRef]

61. Johnston, J.H. Jarosite and akaganéite from White Island volcano, New Zealand: An X-ray and Mössbauer study. *Geochim. Cosmochim. Acta* **1977**, *41*, 539–544. [CrossRef]

62. Bhattacharya, S.; Mitra, S.; Gupta, S.; Jain, N.; Chauhan, P.; Parthasarathy, G. Jarosite occurrence in the Deccan Volcanic Province of Kachchh, western India: Spectroscopic studies on a Martian analog locality. *J. Geophys. Res. Planets* **2016**, *121*, 402–431. [CrossRef]